α - and γ-PVDF: Crystallization kinetics, microstructural variations and thermal behaviour

M.P. Silva [a], V. Sencadas [a], G. Botelho [b], A.V. Machado [c], A.G. Rolo [a], J.G. Rocha [d], S. Lanceros-Mendez [a, *]

[a] Centro de Física, Universidade do Minho, Campus de Gualtar, 4710-057 Braga, Portugal

[b] Dept. de Química, Universidade do Minho, Campus de Gualtar, 4710-057 Braga, Portugal

[c] IPC - Instituto de Polímeros e Compósitos, Dept. de Eng. [a] de Polímeros, Universidade do Minho, Campus de Azurém, 4800-058 Guimarães, Portugal

[d] Dept. Eng. Industrial, Universidade do Minho, 4800-058 Guimarães, Portugal

Keywords:

Crystallization
Avrami
Electroactive
Microstructure
Optical microscopy
kinetics
theory
polymers

Abstract

The kinetics of the isothermal crystallization from the melt of α - and γ-poly (vinylidene fluoride), PVDF, and the corresponding melting behaviour has been investigated. The crystallization kinetics was evaluated on the basis of the theory of Avrami. The variation of the microstructure of the samples crystallized at different temperatures was monitored along time by optical microscopy with polarized light. The correlation between microstructure and kinetic parameters allows tailoring the microstructure of the polymer by choosing specific crystallization conditions. Infrared spectroscopy and Raman

spectroscopy show the appearance of the γ-phase for higher crystallization temperatures.

Introduction

Poly(vinylidene fluoride), PVDF, is the main representative of a family of polymeric materials with interesting scientific and technological properties. This polymer is known for its outstanding electroactive properties, non-linear optical susceptibility and an unusually high dielectric constant among polymers [1].

The electroactive properties of the material heavily depend on the phase content, microstructure and degree of crystallinity of the material, which in turn depend on the processing conditions [2,3]. In particular, the microstructure of α-PVDF plays an important role in the α - to β-phase transformation by stretching [3]. This stretching process is the typical way for obtaining the most common electroactive polymorph [3,4] and deeply influences the properties of the β-phase [5]. Furthermore, in order to prepare polymer/ceramic composites or nanocomposites with the carbon nanotubes or other nanoparticles within the polymeric matrix, it is essential to previously characterize and understand the crystallization properties of the matrix.

Despite the many studies on the electroactive properties of PVDF, copolymers and composites [1-5], there are still a lack of solid information on the crystallization kinetics and its relationship

to the morphology and phases present in the material, an important issue when tailor-made crystallization wants to be achieved. Further, there are some variations on the kinetic crystallization parameters obtained for PVDF [6-10].

Liu et al. [6] studied the crystallization and morphology behaviour of PVDF. They report that the Avrami exponent for pure PVDF is approximately 3 when the Avrami conditions are fulfilled. It is suggested that the growth of spherulites is three dimensional with athermal quench-induced nucleation. They also reported that the half crystallization time ($t_{1/2}$) of PVDF increases with increasing crystallization temperature.

Qiu et al. [7] reported that the crystallization of PVDF is affected by the crystallization temperature and that the average values of the Avrami exponent are around 2.5, indicating that the crystallization of PVDF might correspond to the spherulitic growth with heterogeneous nucleation.

Chiu [8] studied the spherulitic morphology and crystallization kinetics of PVDF. This author found an Avrami exponent of approximately 3 for PVDF and suggested that the crystallization of the polymer occurs in a spherulitic growth with heterogeneous nucleation. Mancarella and Martuscelli [9] investigated the crystallization behaviour of PVDF, reporting that the Avrami exponent ranges between 2.99 and 4.60 and the half crystallization time increases with increasing crystallization temperature. Fan and Zheng [10] studied the miscibility behaviour in blends of poly(methyl methacrylate) and poly(vinylidene fluoride). The results for pure PVDF are in the same range of the work published

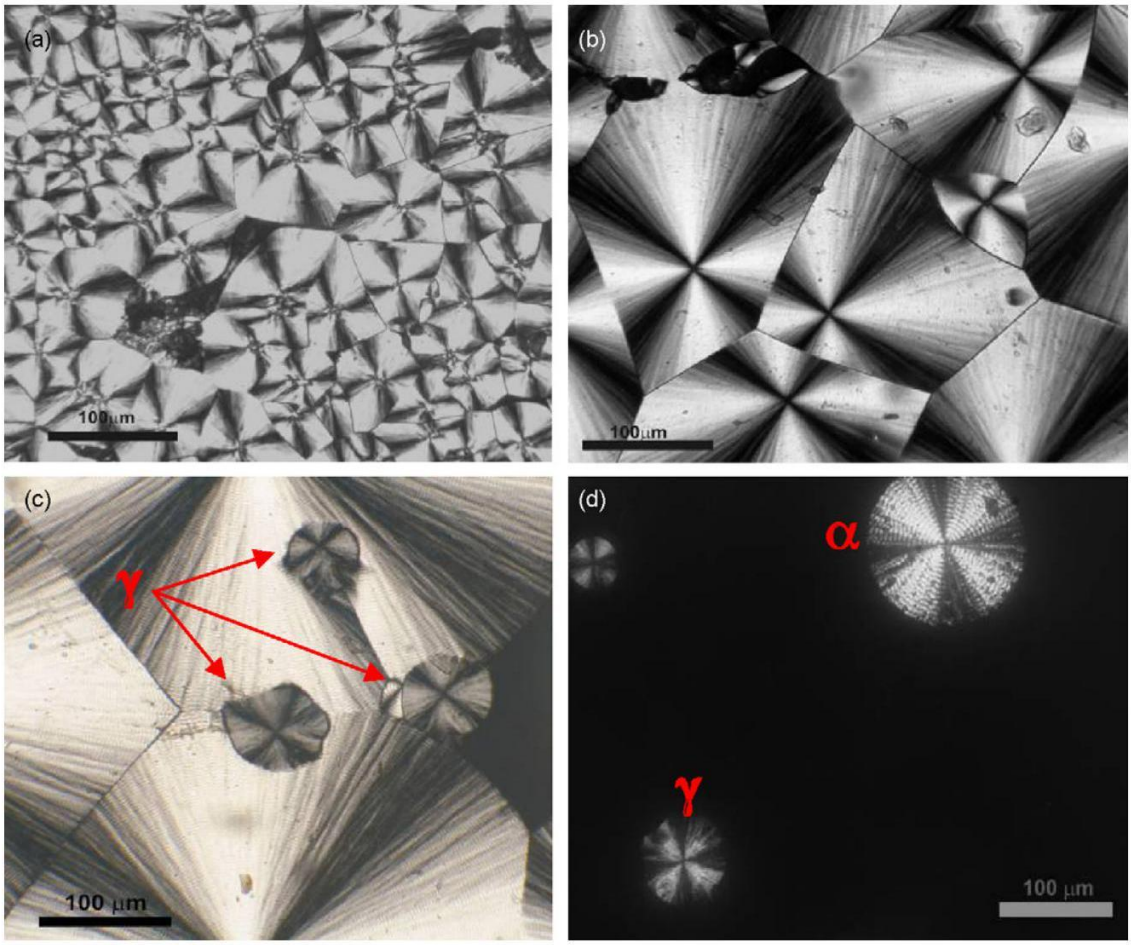

Fig. 1. PVDF samples crystallized at: (a) 150°C, (b) 155°C and (c) 160°C. (d) Snapshot of the crystallization process at 165°C, where the growth of both α - and γ-spherulites from the melt can be observed.
in Ref. [9]. The Avrami exponent decreases with increasing crystallization temperature.

Furthermore, the relationship between the spherulitic microstructure, phase content and crystallization kinetics must be explored in order to achieve a proper characterization, understanding and control of the crystallization process.

The present work studies the kinetics of the isothermal crystallization of PVDF from the melt at different crystallization temperatures by optical microscopy experiments. Differential scanning calorimetry, Raman spectroscopy and infrared spectroscopy have been used in order to identify the crystalline phases present in the samples.

Experimental

Films of α-PVDF with thickness of $\sim 30\mu$ m were obtained by spreading a solution of PVDF (Solef 1100 from Solvay) in N,N-dimethyl formamide (DMF - Merck) on a glass slide. The initial concentration of the solution was 20%(w/w) of PVDF. The system was kept inside an oven at a controlled temperature of 120°C during a period of 60 min . This time was enough to ensure the removal of the solvent by evaporation and the isothermal

crystallization of PVDF. After evaporation of the solvent, the sample was melted at $220°C$ for 10 min , removed from the oven and cooled down at room temperature. The polymer obtained by this procedure is predominantly α-PVDF [1,3].

Isothermal crystallization from the melt was studied using a hot stage Linkam TMS-92 furnace operating in a nitrogen atmosphere. The following procedure was employed for all samples: the samples were melted at $220°C$ and kept at this temperature for 10 min in order to erase the thermal history and remove any residual crystallinity. After this step, the samples were quenched ($30°C min^{-1}$) to the chosen crystallization temperature T_c(150,155,160 and $165°C$). Images of the spherulitic growth during crystallization of PVDF were obtained with an optical microscope with polarized light (Olympus BH-2). The pictures were taken using a Leica DFC-280 camera.

Differential scanning calorimetry (DSC) experiments were performed with a Mettler Toledo DSC 821^e differential scanning calorimeter using 40μ L aluminium pans. Polymer samples were heated from 25 to $200°C$ at a constant heating rate of $10°C min^{-1}$ using high purity argon as a purge gas. The crystalline phase (or phases) present in each sample was confirmed by infrared spectroscopy (Spectrum 100 PerkinElmer apparatus) and Raman spectroscopy (Jobin-Yvon $T64000$ triple-grating spectrometer + CCD detector, excitation 514.5 nm from Ar laser in backscattering).

Results and discussion

Fig. 1a-c shows the final microstructure obtained for samples crystallized at different temperatures. Fig. 1d shows a snapshot of the crystallization process at a temperature of $165°C$, where α - and γ-spherulites grow simultaneously from the melt. Samples crystallized at the lowest temperatures (150 and $155°C$) only show one type of spherulites, corresponding to the α-phase of PVDF [6]. The material crystallized at $150°C$ has the finest microstructure among the samples prepared in this work, due to the faster crystallization. With increasing crystallization temperature the crystallization rate slows down (Fig. 2) and the diameter of the spherulites increases (Fig. 1).

For crystallization temperatures higher than $160°C$, a new type of spherulites emerges in the material. These spherulites are smaller and darker than the ones already present when crystallization at lower temperatures occurs (Fig. 1c and d). These spherulites show the crystallization of PVDF in the γ-phase [6]. Spherulites in the γ-phase are much smaller and enter inside of the α-phase spherulites (Fig. 1c), leaving behind it a comet-like tail that deforms the polymer matrix.

Fig. 2 shows the variation of the radius of the spherulites over time for positively birefringent spherulites. The measurements have been performed during the time in which the spherulites growth independently, with no influence of the neighboring growing spherulites. For the lowest temperatures, the polymer crystallizes faster, giving rise to the smallest spherulites, as

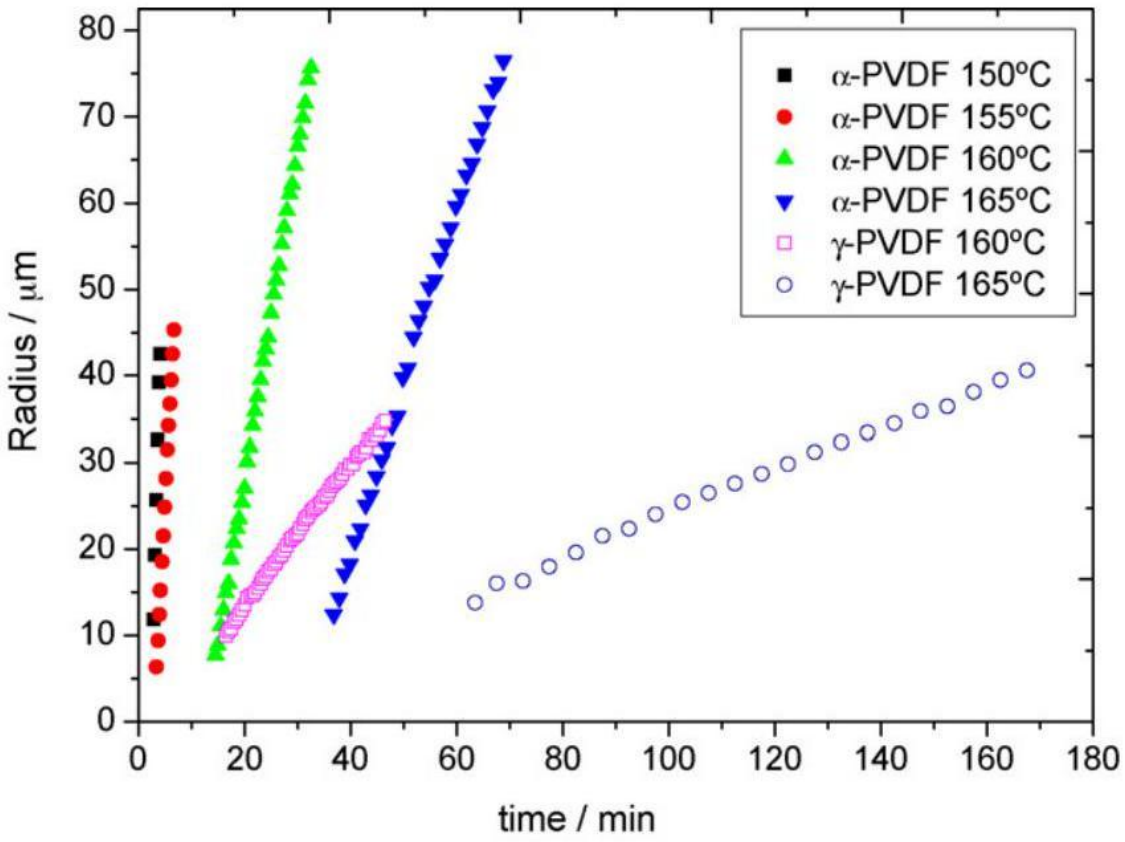

Fig. 2. Spherulitic growth for α - and γ-PVDF spherulites at different crystallization temperatures.

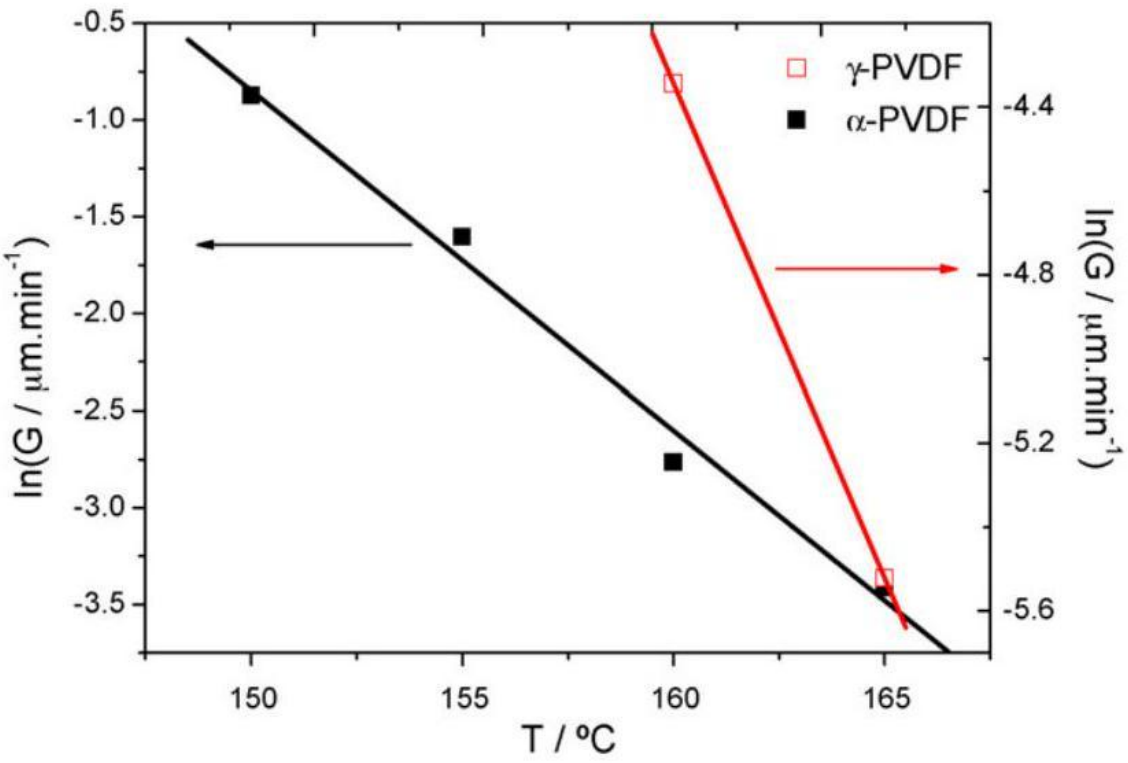

Fig. 3. Crystallization rate, G, of the α - and γ-PVDF spherulites at different temperatures. observed by optical microscopy with polarized light (Fig. 1a). For higher temperatures, the crystallization process is slower and the diameter of the spherulites is larger for both α - and γ-spherulites (Fig. 2).

For each isothermal crystallization temperature under study, the spherulitic radius (R) was observed to increase linearly over time, indicating a constant growth rate throughout the crystallization process. This implies that the concentration of impurities at the growing tips of the lamellae remains constant through the growth process [9]. The γ-phase spherulites show a lower growth rate than the α-phase spherulites, reaching also lower dimensions, when the crystallization is completed (Fig. 2). The main reason for this phenomenon is that the spherulites related to the γ-phase start to appear later, once part of the polymer is already crystallized in the α-phase.

The spherulitic growth rates ($G = dR/dt$) of PVDF (Fig. 3) have been quantitatively determined from the results shown in Fig. 2. The growth rate of the spherulites decreases with increasing crystallization temperature, being the decrease stronger for the γ-phase.

A linear relationship between ln G and temperature is verified for the two types of spherulites. Of course there is a larger uncertainty in the results obtained for the γ-phase spherulites, as these spherulites are observable just for two of the crystallization temperatures. Nevertheless, this linear relationship is the one typically observed in other polymer systems [8,11].

Overall crystallization kinetics

The overall crystallization rate is determined by both the nucleation and growth rates. Usually, the crystallization kinetics is studied by DSC [7]. In this work the study of the kinetic behaviour is based on optical measurements [6,11], as it allows the immediate assessment of the crystallization kinetics and the microstructure and phase evolution of the polymer. From images similar to the ones presented in Fig. 1, taken at regular time intervals during the crystallization process, the fraction (X_t) of the material that crystallizes at a time t was calculated from the evolution of the area of crystallization as a function of time ($\partial A/\partial t$). The rate curves can be processed by integration to determine the relative extent of crystallization as a function of time, i.e. by assuming: $X_t = \frac{\int_0^t (\partial A/\partial t)\partial t}{\int_0^\infty (\partial A/\partial t)\partial t}$,
where the numerator represents the crystallized area at a given time (spherulite filled area of e.g. Fig. 1d) and the denominator is the total area of the fully crystallized material (total area of e.g. Fig. 1d). Fig. 4 displays the evolution of X_t over time for the PVDF samples crystallized different temperatures. In the former experiments, the zero time of the crystallization process was taken when the first spherulite starts to appear in the image.

Plots of the relative crystallinity as a function of time for the α-PVDF spherulites show the sigmoidal shape typical of the isothermal polymer crystallization (Fig. 4, left). Furthermore, the initial slope decreases with increasing crystallization temperature, indicating a progressively slower crystallization rate, as it was also observed in Fig. 3. As a conclusion, increasing crystalliza-

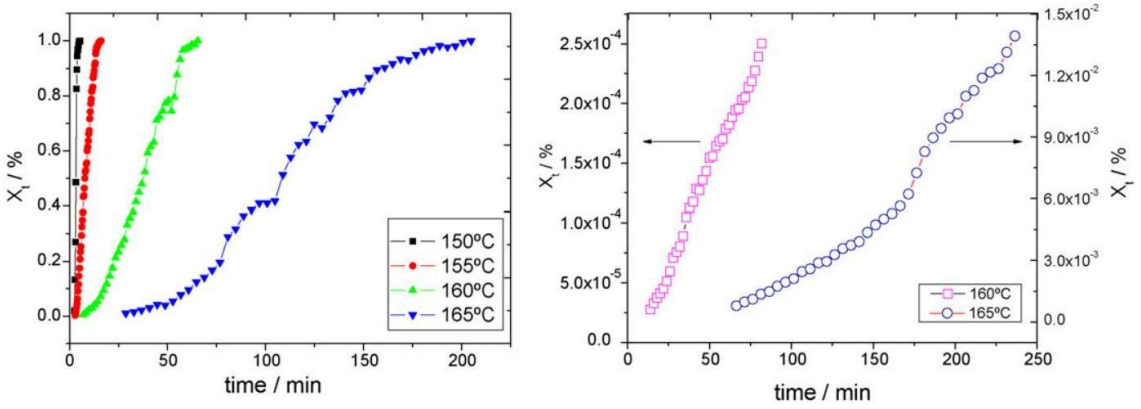

Fig. 4. Crystallization isotherms of α − PVDF (left) and γ − PVDF (right) for the different crystallization temperatures.

Table 1
Avrami parameters obtained from the fittings with Eq. (3), describing the crystallization kinetic of PVDF in the α - and γ-phases upon isothermal crystallization from the melt.

T_C(°C)/ phase	n	$k(\min^{-n})$	$t_{1/2}$(min)
150/ α	3.70	7.45×10^{-3}	3.4
155/ α	2.93	1.52×10^{-3}	8.1
160/ α	2.79	3.18×10^{-5}	36.0

165/ α	3.18	2.29×10^{-7}	109.0
160/γ	1.25	1.60×10^{-6}	31,999
165/γ	2.25	6.36×10^{-8}	1342

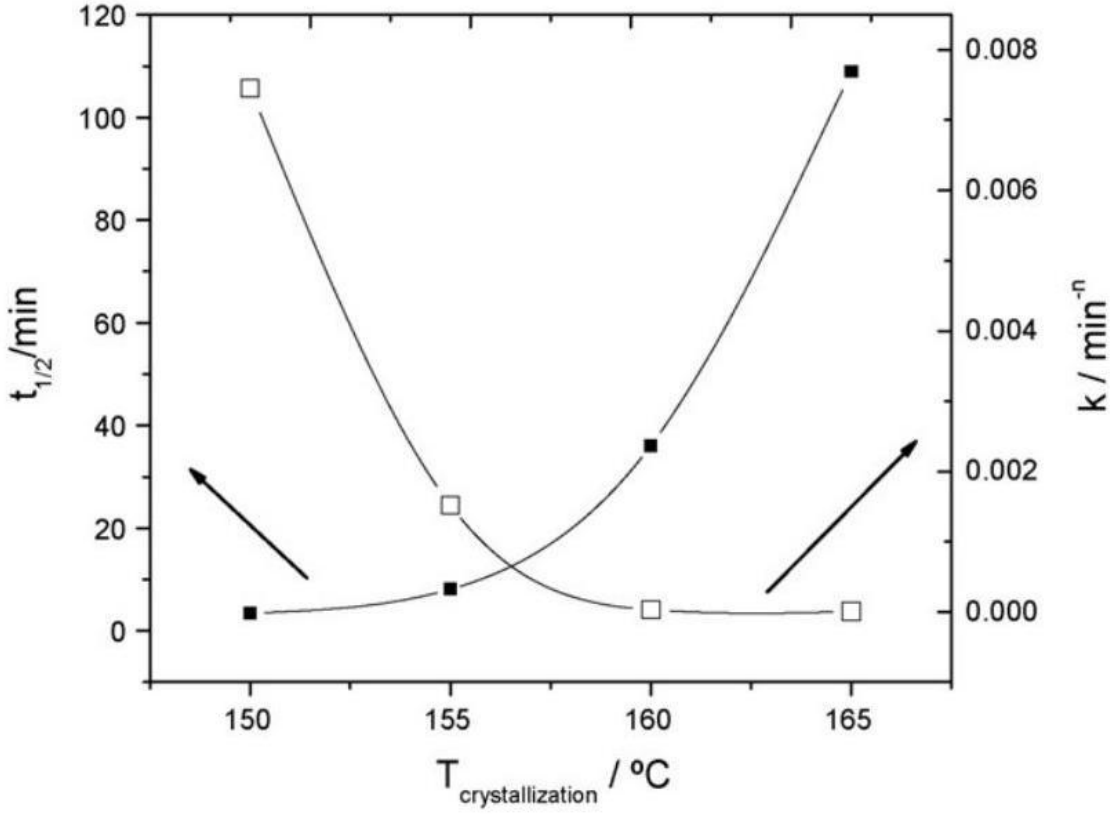

Fig. 5. Crystallization half-time $t_{1/2}$ vs crystallization temperature $T_{\text{crystallization}}$, for isothermal crystallization of PVDF from the melt. tion temperature strongly slows down the overall crystallization kinetics.

The same procedure was adopted for the samples with γ-PVDF spherulites and a similar behaviour as the one observed for the α-phase samples was found. Fig. 4 (right) shows the results for the γ-phase crystallized at 160 and 165°C. For these samples, only the initial steps of crystallization are presented, corresponding to the time at which the γ-phase spherulites grow independently (Fig. 1d). At temperatures above 160°C the samples crystallize in a mixture of α - and γ-phases (Fig. 1c). The crystallization of the γ-phase spherulites, with lower crystallization rates and in smaller relative quantity, is influenced by the growth of the α phase spherulites already present in the polymer when the γ-phase spherulites begin to appear. So, the data presented in Fig. 4a, correspond to the initial part of the sigmoidal curve.

From the isothermal crystallization experiments, the half-time of the crystallization $t_{1/2}$, defined as the time required to attain half of the final crystallinity ($X_t = 0.5$) was calculated. $t_{1/2}$ represents the overall crystallization rate of the process and is governed by

the rates of nucleation and crystal growth [12]. The combined effect of the two rates produces a maximum in the crystallization rate at a temperature between the melting point and the glass transition temperature. This fact gives rise to the so-called bell curve of isothermal crystallization [12]. The half-time of crystallization was determined and is shown in Table 1.

Fig. 5 illustrates the evolution of the $t_{1/2}$ with the crystallization temperature for the α-phase spherulites. As expected, the crystallization half-time decreases with decreasing crystallization temperature, $T_{\text{crystallization}}$, i.e. the crystallization rate increases with super cooling [13]. On the other hand, the crystallization half-time of the γ-phase dramatically decreases with increasing temperature (Table 1). The reason of the different behaviour with respect to the α-phase relies basically in the higher stability and therefore an increasing amount of γ-phase at the higher temperature.

At a macroscopic level, useful constitutive equations describing isothermal crystallization of polymers can be developed. Isothermal crystallization refers to the phenomenon when the spherulite growth process is steady; i.e. the degree of crystallinity (X_t) is independent of the temperature. This can be explicitly stated as:

$$1 - X_t = \exp(-kt^n) \tag{2}$$

where k is the overall crystallization rate constant, containing contributions from both nucleation and growth rate, and n is the Avrami exponent which depends on the nature of the nucleation and growth geometry of the crystals. This equation is commonly known as the Avrami equation of crystallization [14-16].

The plot of

$$\ln[-\ln(1 - X_t)] = n\ln\ t + \ln\ k \tag{3}$$

produces a straight line with intercept and slope given by $\ln\ k$ and n, respectively. Typically, Avrami equation represents correctly only the initial steps of polymer crystallization, characterized by a linear regime (Fig. 4). The spherulites grow outward with a constant radial growth rate until impingement takes place when they stop growing at the intersection with other spherulites. After that, a secondary crystallization process is often observed in the amorphous interstices [8].

Eq. (3) is valid only if the nucleation and growth conditions do not change during the crystallization process [14-16]. Fig. 6 displays the Avrami plots and respective fittings for the α - and γ-PVDF spherulites, respectively, for the different crystallization temperatures.

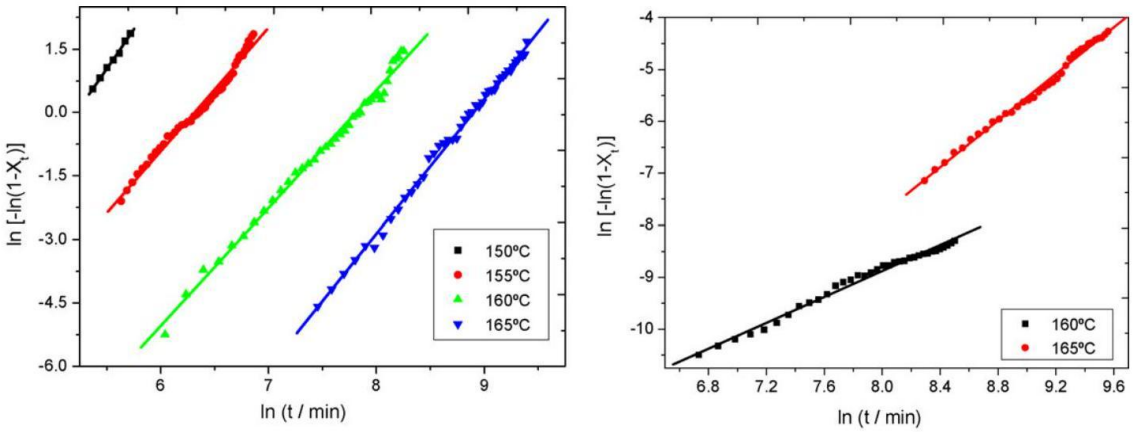

Fig. 6. Crystallization rate at different temperature of spherulites of α-PVDF (left) and γ-PVDF (right).

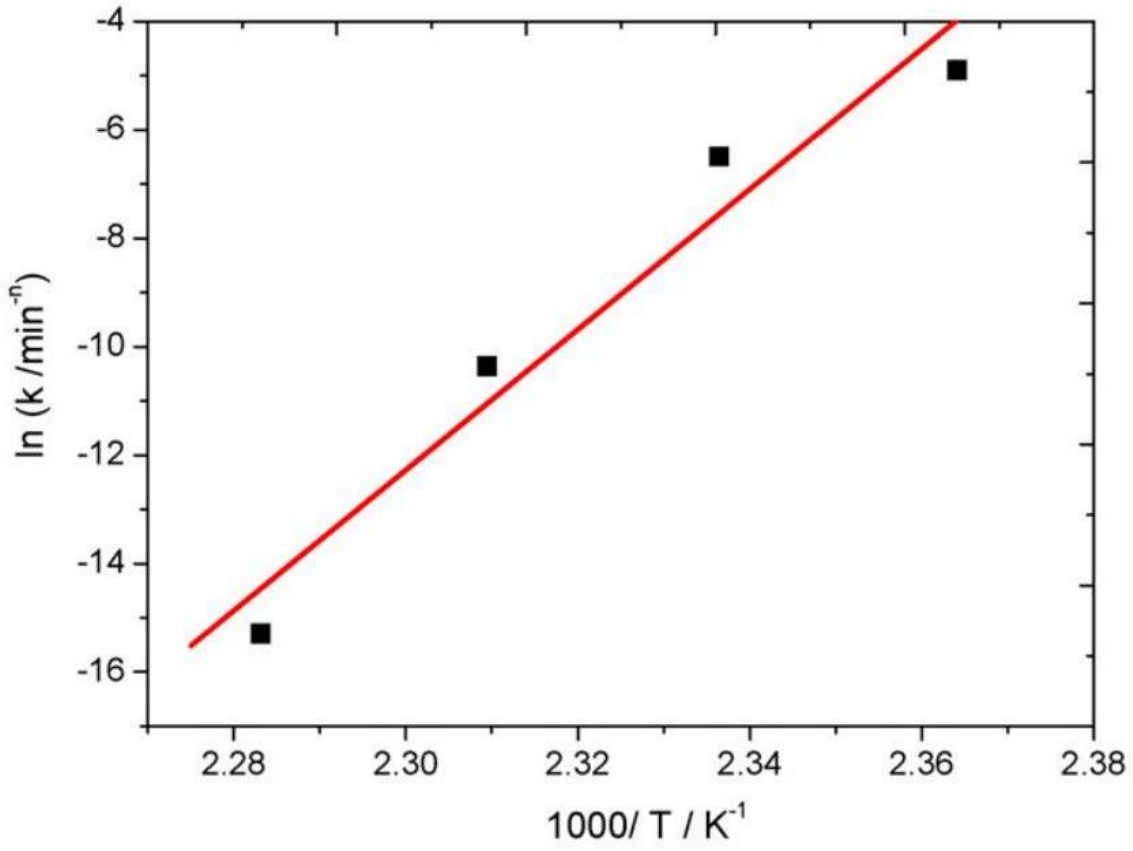

Fig. 7. Plot of the ln of the overall crystallization rate k for the α-PVDF samples against inverse temperature.

The kinetic rate constant, k was calculated by using the relation:

$$k = \frac{\ln 2}{t_{1/2}^{n}} \tag{4}$$

where $t_{1/2}^{n}$ is the half-time crystallization and is defined as the time required to reach half of the final crystallinity.

The linear behaviour observed in Fig. 6 indicates that PVDF behaves according to Eq. (3) for all temperatures. All fittings show linear behaviour with $R > 0.99$ (Fig. 6). Table 1 summarizes the crystallization parameters for the isothermal crystallization of PVDF obtained from the fittings with Eq. (3).

The value of parameter n obtained for α-PVDF crystallized at 150°C is almost 4. This suggests that the growth of the spherulites is three dimensional with thermal quench-induced nucleation [8], in agreement to the results obtained by Mancarella and Martuscelli [9]. For higher crystallization temperatures, the parameter n of α-PVDF decreases from 4 to approximately 3, suggesting that the growth of the spherulites is three dimensional with athermal quench-induced crystallization [8]. Therefore, a change from thermal to athermal quench-induced crystallization with increasing crystallization temperature is observed.

The γ-phase shows different behaviour when compared to the α-PVDF phase. The Avrami exponent n for the sample crystallized at 160°C is 1.25 , indicating that this phase crystallizes in one or two dimensions in a fibrillar structure with athermal quench-induced nucleation [8]. On the other hand, the sample crystallized at 165°C has higher Avrami exponent (2.25), which corresponds to a threedimensional crystallization in a lamellar structure with athermal quench-induced nucleation [8]. So, the change in the value of the parameters reflects the variation in the spherulite architecture from fibrillar to lamellar with increasing crystallization temperature.

The half-time crystallization $t_{1/2}^{n}$ found for γ-PVDF was approximately 31,999 and 1342 min for the isothermal crystallization temperatures of 160 and 165°C, respectively. These values are much higher than the ones found for the α-phase: the crystallization of the γ-phase begins later and the crystallization rate is lower than the one of α-PVDF.

The Avrami model only fits to the experimental results for the primary crystallization, when the spherulites can growth without impingements. For PVDF and for isothermal crystallization temperatures higher than 155°C, the material crystallizes in a co-existence of α - and γ-crystalline phases. When the material is all solidified, the sample is mainly constituted by α-PVDF due to the faster crystallization rate. The high values found for the half-time crystallization of the γ-phase are due both to the fact that the Avrami theory just represents correctly the initial steps of polymer crystallization (initial linear region) and to the lower crystallization rate of the γ-phase. The values found represent a theoretical value based on the Avrami model.

The discussion before just refer to γ-spherulites grown directly from the melt. As it will be shown later, γ-phase material is also achieved by phase transition from α-phase polymer [4,6]. These spherulites are of different nature presenting also different thermal stability (see later).

The activation energy of the crystallization process can be obtained by applying the Arrhenius equation to the overall crystallization rate constant k, containing contributions from both nucleation and growth rate: $k = A\exp\left(-\frac{E_{\mathrm{Act}}}{RT_{\mathrm{crystallization}}}\right)$,

where A is the pre-exponential factor, E_{Act} is the activation energy of the crystallization process and R the ideal gas constant ($R = 8.31$ J mol^{-1} K^{-1}) [7,11]. Fig. 7 shows the ln of the overall crystallization rate against the inverse of the crystallization temperature. The activation energy obtained for the crystallization of the α-phase is 15.58 kJ/mol.

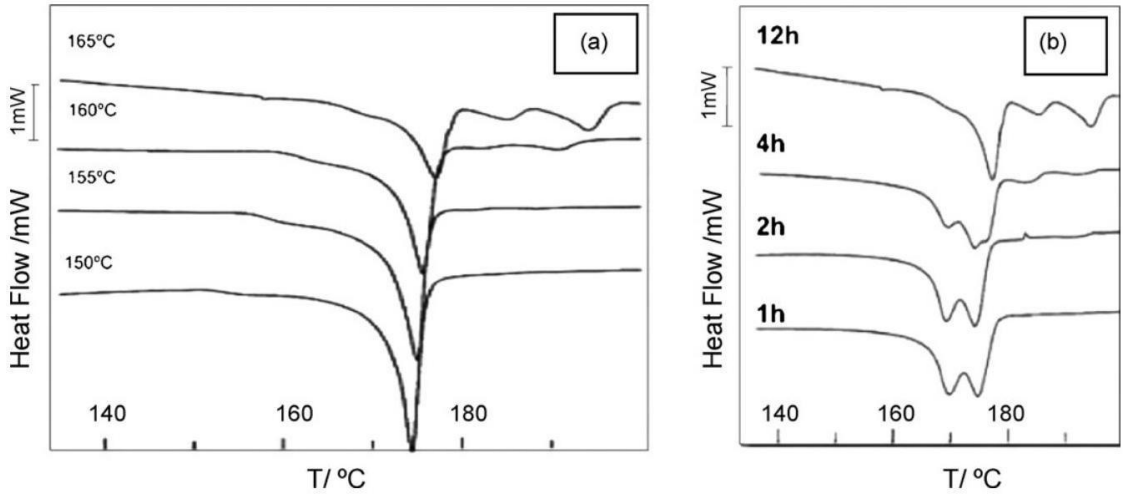

Fig. 8. DSC thermograms for the different samples: (a) crystallization for the same time at different temperatures; (b) crystallization at the same temperatures for different times.

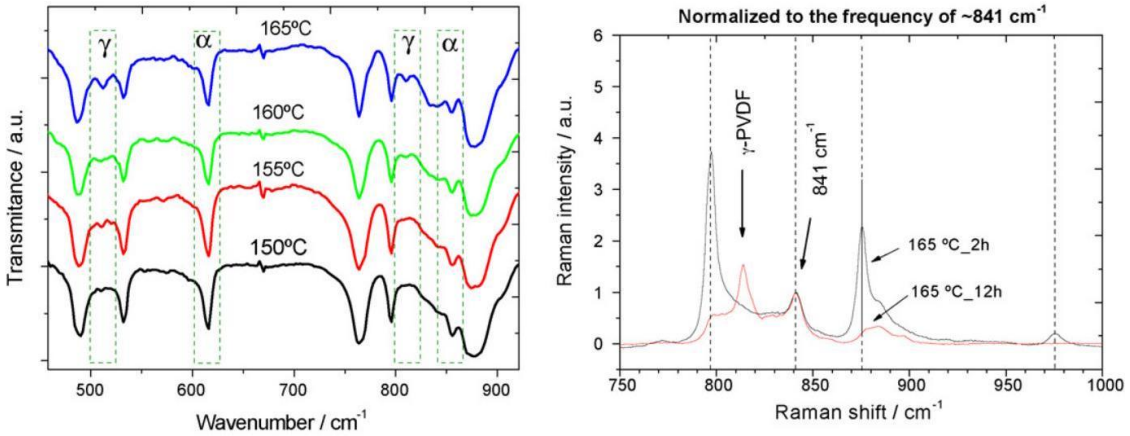

Fig. 9. FTIR results for PVDF samples crystallized at different temperatures (left) and Raman spectra for samples crystallized at 165°C for 2 and 12 h (right). The Raman spectra are normalized to the frequency of ~ 841 cm^{-1}.

Confirmation of the phases obtained under the different conditions

The existence of the different phases and their nature can be also confirmed by differential scanning calorimetry (DSC), far infrared spectroscopy and Raman spectroscopy. DSC thermograms for samples crystallized for the same time at different temperatures and for

samples crystallized at the same temperatures for different times are presented in Fig. 8 a and b , respectively. The appearance of the γ-polymorph is confirmed by the far infrared and Raman spectra (Fig. 9).

The degree of crystallinity of the samples slightly decreases for increasing temperatures, as can be deduced from the area of the melting peak of the DSC curves (Fig. 8a). For crystallization temperatures of 160°C and higher, two melting peaks above the melting temperature of the α-phase material are observed. The two peaks correspond to the two types of γ-phase polymer present in the samples, showing different thermal stabilities: γ-phase obtained from transformation of α-phase material and γ-phase directly crystallized from the melt [4,6]. For samples crystallized at different times (Fig. 8b), crystallization for 1 h leads to a double peak structure corresponding to the α-phase crystallization. The lower temperature peak corresponds to ill crystallized crystallites with a large amount of defects. Increasing crystallization times leads progressively to a decrease of the lower temperature peak and an appearance of the γ phase peaks, indicating the existence of inter-conversion between these phases (phase transformation). The α-phase peak does not significantly change upon crystallization time.

The infrared spectra for samples crystallized at different temperatures for 12 h confirmed that the material obtained after crystallization at lower temperatures is exclusively in the α-phase [17]. The presence of the γ-phase is only detected for the samples crystallized at temperatures of 160°C and higher (Fig. 9, left). The amount of γ-phase also depends on the crystallization time (Fig. 9, right). As observed in Fig. 9, left, increasing crystallization time at 165°C induce the emerging of the γ-phase, as indicated by the corresponding mode at 810 cm^{-1} [17,18]. The γ-phase at this temperature appears directly by crystallization from the melt and not by phase transformation from the α-phase. These results confirm the previously discussed optical and DSC data.

Conclusions

Poly(vinylidene fluoride) was obtained by isothermal crystallization from the melt at different crystallization temperatures and the growth kinetics was evaluated from optical experiments. For lower temperatures, the rapid growth of the spherulites results on smaller spherulites in the final crystallized samples. For crystallization at temperatures below 160°C the samples contain exclusively PVDF in the α-phase. For crystallization at higher temperatures γ phase spherulites also appear in the samples. The crystallization of the γ-phase also depends on the crystallization time. The existence of the different phases is confirmed by Raman spectroscopy and infrared spectroscopy. The γ-phase spherulites can be of two types: those directly crystallized from the melt and those transformed from the α-phase material. The different types of spherulites show different thermal stability. The Avrami equation can be applied to both α - and γ-spherulites. The crystallization morphology changes depending on the crystallization temperature: the α-phase spherulites change from thermal to athermal quench-induced crystallization with increasing crystallization temperature; the γ-phase spherulites change spherulite architecture from fibrillar to lamellar with increasing crystallization temperature.

Acknowledgments

The authors thank the Portuguese FCT Grants PTDC/CTM/ 73030/2006, PTDC/CTM/69316/2006 and NANO/NMed-SD/ 0156/2007. V.S. thanks the FCT for the SFRH/BPD/63148/2009 grant.

References

[1] A.J. Lovinger, in: D.C. Basset (Ed.), Developments in Crystalline Polymers, Applied Science Publications, London, 1981.
[2] A. Salimi, A.A. Yousefi, Polym. Test. 22 (2003) 699.
[3] V. Sencadas, R. Gregorio Jr., S. Lanceros-Méndez, J. Macromol. Sci., Part B: Phys. 48 (2009) 514.
[4] R. Gregorio Jr., E.M. Ueno, J. Mater. Sci. 34 (1999) 4489.
[5] M.C. Branciforti, V. Sencadas, S. Lanceros-Méndez, R. Gregorio Jr., J. Polym. Sci. Part B: Polym. Phys. 45 (2007) 2793.
[6] J. Liu, Z. Qiu, B.J. Jungnickel, J. Polym. Sci. Part B: Polym. Phys. 43 (2005) 287.
[7] Z. Qiu, C. Yan, J. Lu, W. Yang, Macromolecules 40 (2007) 5047.
[8] H.J. Chiu, J. Polym. Res. 9 (2002) 169.
[9] C. Mancarella, E. Martuscelli, Polymer 18 (1977) 1240.
[10] W. Fan, S. Zheng, J. Polym. Sci. Part B 45 (2007) 2580.
[11] Y. Long, R.A. Shanks, Z.H. Stachurski, Prog. Polym. Sci. 20 (1995) 651.
[12] Y.S. Hu, M. Rogunova, D.A. Schiraldi, A. Hiktner, E. Baer, J. Appl. Polym. Sci. 86 (2002) 98.
[13] G.Z. Papageorgiou, G.P. Karayannidis, Polymer 42 (2001) 2637.
[14] M. Avrami, J. Chem. Phys. 7 (1939) 1103.
[15] M. Avrami, J. Chem. Phys. 8 (1940) 212.
[16] M. Avrami, J. Chem. Phys. 9 (1941) 177.
[17] S. Lanceros-Mendez, J.F. Mano, A.M. Costa, V.H. Schimidt, J. Macromol. Sci. Phys. B 40 (2001) 517.
[18] R. Gregorio Jr., R.C. Capitão, J. Mater. Sci. 35 (2000) 299.